

AD-A054 030

AEROSPACE CORP EL SEGUNDO CALIF IVAN A GETTING LABS F/G 7/4
MECHANISMS OF ENERGY TRANSFER IN DEUTERIUM FLUORIDE SYSTEMS. (U)
APR 78 R L WILKINS F04701-77-C-0078

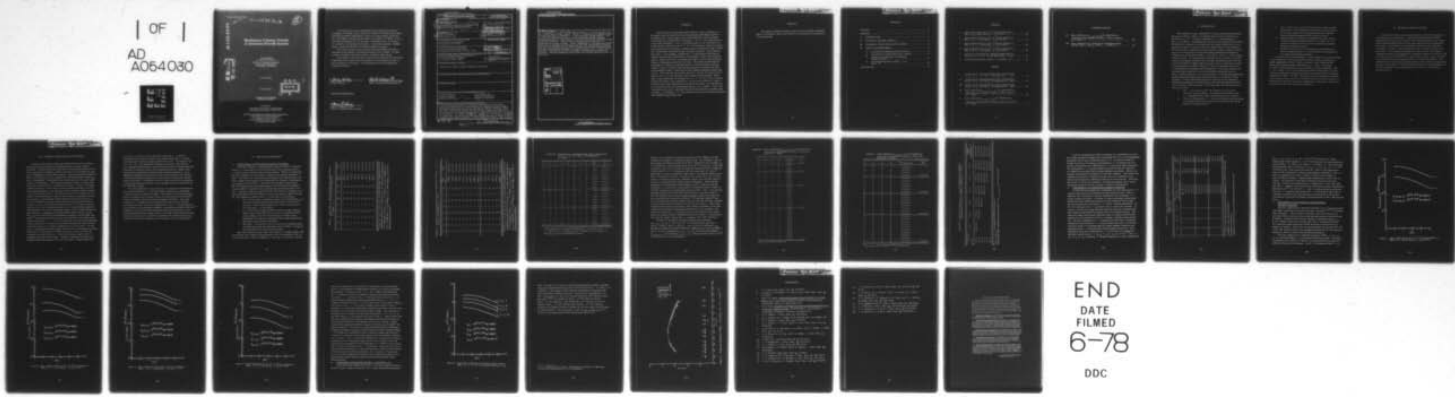
UNCLASSIFIED

TR-0078(3603)-2

SAMSO-TR-78-85

NL

| OF |
AD
A054 030



END
DATE
FILMED
6-78
DDC

AD A 054030

8045617

FOR FURTHER TRAN

2002
2

Mechanisms of Energy Transfer in Deuterium Fluoride Systems

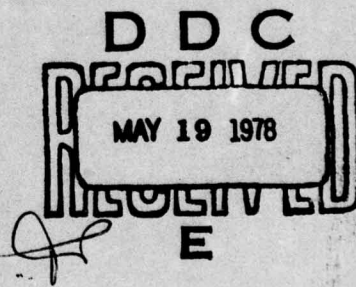
AD No.

DDC FILE COPY

R.L.WILKINS
Aerophysics Laboratory
The Ivan A. Getting Laboratories
The Aerospace Corporation
El Segundo, Calif. 90245

13 April 1978

Interim Report



APPROVED FOR PUBLIC RELEASE;
DISTRIBUTION UNLIMITED

Prepared for

AIR FORCE WEAPONS LABORATORY
Kirtland Air Force Base, N. Mex. 87117

SPACE AND MISSILE SYSTEMS ORGANIZATION
AIR FORCE SYSTEMS COMMAND
Los Angeles Air Force Station
P.O. Box 92960, Worldway Postal Center
Los Angeles, Calif. 90009

This interim report was submitted by The Aerospace Corporation, El Segundo, CA 90245, under Contract No. F04701-77-C-0078 with the Space and Missile Systems Organization, Deputy for Advanced Space Programs, P.O. Box 92960, Worldway Postal Center, Los Angeles, CA 90009. It was reviewed and approved for The Aerospace Corporation by W. R. Warren, Jr., Director, Aerophysics Laboratory. Lieutenant Dara Batki, SAMSO/YCPT, was the project officer for Advanced Space Programs.

This report has been reviewed by the Information Office (OI) and is releasable to the National Technical Information Service (NTIS). At NTIS, it will be available to the general public, including foreign nations.

This technical report has been reviewed and is approved for publication. Publication of this report does not constitute Air Force approval of the report's findings or conclusions. It is published only for the exchange and stimulation of ideas.

Dara Batki
Dara Batki, Lt, USAF
(Project Officer

Robert W. Lindemuth
Robert W. Lindemuth, Lt Col, USAF
Chief, Technology Plans Division

FOR THE COMMANDER

Floyd R. Stuart
FLOYD R. STUART, Col, USAF
Deputy for Advanced Space Programs

UNCLASSIFIED

SECURITY CLASSIFICATION OF THIS PAGE (When Data Entered)

19) REPORT DOCUMENTATION PAGE			READ INSTRUCTIONS BEFORE COMPLETING FORM	
1. REPORT NUMBER 18 SAMSO TR-78-85	2. GOVT ACCESSION NO.	3. RECIPIENT'S CATALOG NUMBER		
4. TITLE (and Subtitle) MECHANISMS OF ENERGY TRANSFER IN DEUTERIUM FLUORIDE SYSTEMS			5. TYPE OF REPORT & PERIOD COVERED 9 Interim Rept.	
6. AUTHOR(s) 10 Roger L. Wilkins			7. PERFORMING ORG. REPORT NUMBER 14 TR-0078(3603)-2	
8. CONTRACT OR GRANT NUMBER(s) 15 F04701-77-C-0078			9. PERFORMING ORGANIZATION NAME AND ADDRESS The Aerospace Corporation El Segundo, Calif. 90245	
10. PROGRAM ELEMENT, PROJECT, TASK AREA & WORK UNIT NUMBERS			11. CONTROLLING OFFICE NAME AND ADDRESS Air Force Weapons Laboratory Kirtland Air Force Base, N. Mex. 87117	
12. REPORT DATE 11 13 April 1978			13. NUMBER OF PAGES 30 12 36p.	
14. MONITORING AGENCY NAME & ADDRESS (if different from Controlling Office) Space and Missile Systems Organization/ Air Force Systems Command Los Angeles, Calif. 90009			15. SECURITY CLASS. (of this report) Unclassified	
16. DISTRIBUTION STATEMENT (of this Report) Approved for public release; distribution unlimited.				
17. DISTRIBUTION STATEMENT (of the abstract entered in Block 20, if different from Report)				
18. SUPPLEMENTARY NOTES				
19. KEY WORDS (Continue on reverse side if necessary and identify by block number) Chemical Kinetics Energy Transfer Deuterium Fluoride delta for to Rate Coefficients Vibrational Relaxation Rotational Relaxation				
20. ABSTRACT (Continue on reverse side if necessary and identify by block number) A three-dimensional trajectory study has been employed to determine temperature-dependent rate coefficients for the important energy-transfer and deactivation processes that occur in $DF(v_1) + DF(v_2)$ collisions. From this study, it was predicted that the $v \rightarrow v$ energy-transfer processes occur by means of $\Delta v = \pm 1$ transitions and that the rate coefficients for the $v \rightarrow v$ processes $DF(v_1 = 1) + DF(v_2) \rightarrow DF(v_1' = 0) + DF(v_2' = v_2 + 1)$ with $v_2 = 1$ through 5, respectively, decrease with increasing vibrational quantum number v . The computed rate coefficients for the $v \rightarrow v$ processes were $k(v_1 = 1, v_2 = 1;$				

DD FORM 1473
(FACSIMILE)

409 944 to

V1' - V2'
UNCLASSIFIED

SECURITY CLASSIFICATION OF THIS PAGE (When Data Entered)

JOB

UNCLASSIFIED

SECURITY CLASSIFICATION OF THIS PAGE(When Data Entered)

19. KEY WORDS (Continued)

20. ABSTRACT (Continued)

$v'_1 = 0, v'_2 = 2) = 1.3 \times 10^{13} \text{ cm}^3/\text{mole sec}$ and $k(v_1 = 1, v_2; v'_1 = 0, v'_2 = v_2 + 1) = (1.6 f)^{1-v_2} k(1, 1; 0, 2)$ at 300 K. These $v \rightarrow v$ processes correspond to near-resonant vibration-to-vibration ($v \rightarrow v$) intermolecular energy transfer. The $v \rightarrow R$ energy-transfer processes occur by converting multiple quanta of vibrational energy of a vibrationally excited DF molecule into rotational energy of the same molecule. This process corresponds to nonresonant $v \rightarrow R$ intramolecular energy transfer. These multiquantum $v \rightarrow R$ transitions provide more ways to distribute the vibrational energy of the vibrationally excited DF molecule into rotational energy and thereby populate its high rotational states. The high rotational quantum states are quickly relaxed by $R \rightarrow v$ processes and by fast $v \rightarrow R$ processes in which even higher rotational quantum states are produced. The high rotational quantum states are relaxed slowly by $R \rightarrow (R', T)$ processes.

ACCESSION for	
ATR	White Section <input checked="" type="checkbox"/>
DOC	Buff Section <input type="checkbox"/>
UNANNOUNCED <input type="checkbox"/>	
JUSTIFICATION.....	
BY.....	
DISTRIBUTION/AVAILABILITY CODES	
Dist. AVAIL. and/or SPECIAL	
A	

UNCLASSIFIED

SECURITY CLASSIFICATION OF THIS PAGE(When Data Entered)

SUMMARY

This trajectory study predicts that, in $\text{DF}(v_1) + \text{DF}(v_2)$ collisions, $v \rightarrow v$ processes occur by intermolecular energy exchange with single-quantum v transitions, and $v \rightarrow R$ processes occur by intramolecular energy-transfer mechanisms with multiquantum v transitions. The $v \rightarrow v$ rate coefficients decrease with increasing v . The $v \rightarrow v$ processes are in near-resonance with energy defects of less than 100 cm^{-1} . In $v \rightarrow R$ processes, which are nonresonant energy-transfer processes, several quanta of vibrational energy of $\text{DF}(v)$ are converted into rotational energy of the same molecule. This study predicts that $v \rightarrow v$ up-pumping, coupled with $v \rightarrow R$ deactivation with large ΔJ changes, provides the mechanisms to produce high J -states in DF chemical lasers. Both $R \rightarrow R'$ and $R \rightarrow T$ transfer processes occur in rotational deactivation of rotationally excited DF molecules. This study predicted that the probability of rotational deactivation decreases with increasing rotational quantum number J and that single rotational quantum transitions are much more probable at high J -values than are the multiple rotational quantum transitions. This study indicates that DF dimers do not have to be formed to explain the fast $v \rightarrow R$ self-relaxation rates reported experimentally. In this paper, rate coefficients are provided for $v \rightarrow v$, $v \rightarrow R$, and $R \rightarrow (R', T)$ energy-transfer processes; when employed in a rotational nonequilibrium computer program, these rate coefficients can be used to calculate $v \rightarrow R$ rates that can be compared directly with experimental results, when available. These rate coefficients were used to calculate vibrational self-relaxation quenching rates for $\text{DF}(v_1 = 1)$ and $\text{HF}(v_1 = 1)$. The results were found to be in good agreement with available experimental data.

PREFACE

The author is indebted to Karen Foster for her invaluable assistance with the calculations, and to Anne Gwash for her assistance in preparation of the manuscript.

CONTENTS

SUMMARY	1
PREFACE	3
I. INTRODUCTION.....	7
II. POTENTIAL ENERGY SURFACE	9
III. CLASSICAL TRAJECTORY CALCULATIONS	11
IV. RESULTS AND DISCUSSION.....	13
A. Vibrational-to-Rotational Energy Transfer.....	13
B. Vibrational-to-Vibrational Energy Transfer	21
C. Rotational-to-Rotational Translational Energy Transfer	23
D. Vibrational Relaxation of DF($v_1 = 1$) by DF($v_2 = 0$)	28
REFERENCES	33

FIGURES

1.	Rate Coefficients for $R \rightarrow (R', T)$ Energy Transfer of $DF(v_1 = 0, J_1 = 20)$ by $DF(v_2 = 0, J_2)$ vs $10^3/T$	24
2.	Rate Coefficients for $R \rightarrow (R', T)$ Energy Transfer of $DF(v_1 = 0, J_1 = 15)$ by $DF(v_2 = 0, J_2)$ vs $10^3/T$	25
3.	Rate Coefficients for $R \rightarrow (R', T)$ Energy Transfer of $DF(v_1 = 0, J_1 = 10)$ by $DF(v_2 = 0, J_2)$ vs $10^3/T$	26
4.	Rate Coefficients for $R \rightarrow (R', T)$ Energy Transfer of $DF(v_1 = 0, J_1 = 5)$ by $DF(v_2 = 0, J_2)$ vs $10^3/T$	27
5.	Total Rate Coefficients for Rotational Deactivation of $DF(v_1 = 0, J_1 = 5, 10, 15, \text{ and } 20)$ by $DF(v_2 = 0, J_2)$	29
6.	Vibrational Relaxation of $DF(v_1 = 1)$ by $DF(v_2 = 0)$	31

TABLES

I.	Vibrational-to-rotational detailed rate coefficients for $DF(v_1 = 1, J_1 = 3) + DF(v_2 = 0)$ collisions at $T = 300 K$	14
II.	Vibrational-to-rotational detailed rate coefficients for $DF(v_1 = 2, J_1 = 3) + DF(v_2 = 0)$ collisions at $T = 300 K$	15
III.	Vibrational-to-rotational detailed rate coefficients for $DF(v_1 = 3, J_1 = 3) + DF(v_2 = 0)$ collisions at $T = 300 K$	16
IV.	Rate coefficients $k_{v_1, v_2; v'_1, v'_2}$ for vibrational-to- rotational energy transfer in $DF(v_1) + DF(v_2)$ collisions at $T = 300 K$	18
V.	Rate coefficient k_{v_1, v_2, v'_1, v'_2} for vibrational-to- rotational energy transfer in $DF(v_1) + DF(v_2)$ collisions at $T = 300 K$	19

TABLES (Continued)

VI.	Rate coefficients $k_{v_1, v_2; v'_1, v'_2}$ for vibrational-to-rotational energy transfer in $DF(v_1) + DF(v_2)$ collisions at $T = 300$ K	20
VII.	Rate coefficients for vibrational-to-vibrational energy transfer $DF(v_1) + DF(v_2) \rightarrow DF(v_1 - 1) + DF(v_2 + 1)$	22

I. INTRODUCTION

Measurements of rate coefficients for energy-transfer and deactivation processes in $\text{DF}(v_1) + \text{DF}(v_2 = 0)$ collisions have not been reported in the literature for $v_1 > 2$. The rate coefficient for $v \rightarrow v$ energy transfer in $\text{DF}(v_1 = 2) + \text{DF}(v_2 = 0)$ collisions has been measured at temperatures between 295 and 720 K by means of the shock-tube laser-induced fluorescence technique¹ and at 300 K by means of the laser-induced fluorescence technique.² For the most part, experimental measurements for $\text{DF}(v_1) + \text{DF}(v_2)$ systems have been concerned only with the temperature-dependent quenching-rate coefficient for deactivation of $\text{DF}(v_1 = 1)$ by $\text{DF}(v_2 = 0)$ by a $v \rightarrow (R, T)$ energy-transfer process. The experimental techniques used to measure rate coefficients for vibrational relaxation from the upper vibrational levels of HF are much more difficult to apply to DF for several reasons, which have been discussed adequately by Smith³ and Kwok.⁴ There is a definite need for both v - and temperature-dependent rate coefficients for the energy-transfer and deactivation processes that occur from the higher vibrational levels in $\text{DF}(v_1) + \text{DF}(v_2)$ collisions. In a previous paper,⁵ we discussed the important energy-transfer and deactivation processes that occur in $\text{HF}(v_1) + \text{HF}(v_2)$ collisions. A three-dimensional trajectory study was used to determine temperature-dependent rate coefficients for the important mechanisms that occur in $\text{HF}(v_1) + \text{HF}(v_2)$ systems. From that study, the following conclusions were drawn:

1. The $v \rightarrow v$ processes in $\text{HF} + \text{HF}$ collisions occur by intermolecular energy exchange. The most probable paths for this $v \rightarrow v$ exchange involve single vibrational quantum transitions.
2. The rate coefficients for $v \rightarrow v$ processes decrease with increasing v , and most such processes are in near-resonance with energy defects of less than 100 cm^{-1} .

3. The $v \rightarrow R$ processes occur by intramolecular energy-transfer mechanisms. The vibrationally excited HF molecule converts one or more quanta of its vibrational energy into rotational energy, thereby populating its high rotational states.
4. The probability of rotational de-excitation decreases with increasing rotational quantum numbers J . At high J , $\Delta J = \pm 1$ rotational transitions are much more probable than multiple rotational quantum transitions.
5. HF dimers do not have to be formed at room temperature or above to explain the fast $v \rightarrow R$ self-relaxation rates measured by various experimental techniques.

A trajectory study was undertaken to verify that the conclusions reached for the mechanisms of energy transfer in $HF(v_1) + HF(v_2)$ collisions are equally applicable to $DF(v_1) + DF(v_2)$ collisions and to determine the temperature-dependent rate coefficients for $v \rightarrow v$ and $v \rightarrow (R, T)$ and $R \rightarrow (R', T)$ energy-transfer processes in $DF(v_1) + DF(v_2)$ collisions. The $v \rightarrow (R, T)$ and $R \rightarrow (R', T)$ rate coefficients provided in this paper are used to calculate temperature-dependent quenching-rate coefficients for vibrational deactivation of $DF(v = 1)$ by DF . In Section II, the semiempirical treatment of the potential energy surface for DF - DF collisions is briefly reviewed. In Section III, the classical trajectory calculations are discussed. Results and discussions of this study are given in Section IV.

II. POTENTIAL ENERGY SURFACE

The potential energy surface employed here for DF-DF interactions is constructed from two functions: a London-Eyring-Polanyi-Sato (LEPS) potential energy function for the short-range interactions and a point charge, dipole-dipole potential function for the long-range interactions between the four atoms. The method of constructing this surface has been described previously⁵ for HF(v₁) + HF(v₂) interactions and, therefore, will not be repeated here. The resulting semiempirical surface for HF + HF collisions compared favorably with ab initio SCF calculations reported by Yarkony et al.⁶ and with results of the electron gas method used by Parker, Snow, and Pack⁷ to calculate intermolecular potentials between closed-shell systems. The method used to construct this potential-energy surface produces enough of the attractive well in DF(v₁) + DF(v₂) collisions to provide a valid calculation of the energy-transfer and deactivation processes that occur in deuterium fluoride systems.

III. CLASSICAL TRAJECTORY CALCULATIONS

The quasi-classical procedure described by Raff et al.⁸ was used to examine the collision dynamics of diatomic-diatomc energy-transfer processes. The Hamiltonian that describes the four-particle system is written in generalized coordinates, and the resulting set of 18 Hamiltonian equations is integrated on a CDC 7600 computer. The initial vibrational states of $DF(v_1, J_1)$ and $DF(v_2, J_2)$ were assigned the vibrational quantum numbers v_1 and v_2 , respectively. Calculations were made with values of v_1 and v_2 that varied from 0 through 6. The rotational quantum numbers J_1 and J_2 were Monte-Carlo selected for the calculations involving $v \rightarrow v$ and $v \rightarrow R$ energy-transfer processes. For $R \rightarrow (R', T)$ energy-transfer processes, the rotational quantum number J_1 was assigned, and the rotational quantum number J_2 was Monte-Carlo selected. The initial values of the coordinates in each collision are determined by means of a fixed relative translational energy of the reactants, a chosen initial relative separation between the centers of mass of the diatomic molecules; chosen values of the vibrational quantum numbers v_1 and v_2 ; and randomly selected values of the rotational quantum numbers J_1 and J_2 , the impact parameter, the vibrational phase angles of both molecules, two sets of orientational angles, and the rotational planes of both molecules. Averaging over initial internal states of $DF(v_1, J_1)$ and $DF(v_2, J_2)$ was carried out by the technique described by Porter, Raff, and Miller.⁹ For excited vibrational states, the calculation of the initial values of the momenta P_i ($i = 1, \dots, 9$) is more difficult, since the initial amplitudes of both molecules are no longer the classical turning points, and the internal momentum vectors are no longer perpendicular to the bond axis. For this case, a method based on Euler angles was used that was adequately described by Raff et al.⁸ The distance R between the center of mass of the two DF molecules was taken to be 8 a.u. This value is large enough to ensure a negligible initial interaction energy. Relative translational energies were assigned values that ranged from 0.5 to 6 kcal/mole. Approximately 200

trajectories were run for each initial set of parameters. A uniform distribution was used for the square of the impact parameter b . All runs were made with a maximum impact parameter of 2.5 \AA . The step size was $5.7 \times 10^{-17} \text{ sec}$. The integration technique by Emanuel, which has not been reported in the literature, proved to be faster than the Runge-Kutta-Gill procedure,¹⁰ with the accuracy of the integration tested by changes in the step size and by integration backward along selected trajectories. As an additional verification of numerical accuracy, each trajectory was checked at each point along the trajectory for conservation of total energy and total angular momentum. Computation time for a single trajectory was dependent on the initial parameters but was, on the average, about 6 sec/trajectory on the CDC 7600 computer.

The final properties of each trajectory were analyzed to determine the nature of the collision, i.e., the total angular momentum and vibrational-rotational energy of both DF molecules. The partition of the internal energy between vibrational and rotational energy was determined from the internal energy of each DF molecule and its total angular momentum. The actual technique for calculating the partitioning of the internal energy has been described previously¹¹ and is not repeated here. The $v \rightarrow v$ energy-transfer cross sections were calculated by Method 2, described previously by Wilkins.¹² In Method 2, it is assumed that vibrational energy is transferred in every collision and that only one quantum state is accessible in the transfer process. The energy-transfer cross sections and specific rate coefficients were calculated by means of the equations given by Karplus, Porter, and Sharma.¹³

IV. RESULTS AND DISCUSSION

A. VIBRATIONAL-TO-ROTATIONAL ENERGY TRANSFER

In HF-HF collisions, a recent trajectory study by Wilkins⁵ concluded that the $v \rightarrow v$ processes occur by intermolecular energy exchange and the $v \rightarrow R$ processes by intramolecular energy exchange. Wilkins concluded that HF dimer formation is not required to explain the vibrational relaxation of HF($v = 1$) by HF($v = 0$). This trajectory calculation also indicates that a collision complex is not formed for the typical DF-DF collision in the temperature range at or above 300 K. This trajectory calculation shows that, in DF*-DF collisions, the vibrational energy of the vibrationally excited DF molecule (DF*) is transferred into rotational energy of the same DF* molecule. A similar result was reported for HF*-HF collisions.⁵ Specific $v \rightarrow R$ rate coefficients for DF-DF collisions at 300 K are given in Tables I through III. The qualitative results of these $v \rightarrow R$ processes are as follows:

1. One or more quanta of vibrational energy of the incident DF(v_1, J_1) molecule is transferred into rotational energy of the same DF molecule. There is little change in the internal energy state of the target DF($v_2 = 0, J_2$) molecule.
2. In $v \rightarrow R$ processes involving DF-DF collisions, high rotational states of the incident DF(v_1, J_1) molecule are populated with the energy change across the reaction having a smaller energy defect than would have been predicted if both reagent and product DF species were assumed rotationless.
3. Since the $v \rightarrow R$ processes occur by conversion of multiple quanta of vibrational energy into rotational energy, the DF($v = 0$) species can be formed in very high rotational states.

Since the rotational energy of DF at any value of J is slightly higher than one-half that of HF, higher rotational states of DF* are populated in DF* collisions than of HF* in HF*-HF collisions. The value of J , however, will not

TABLE I. Vibrational-to-rotational detailed rate coefficients for
 $DF(v_1 = 1, J_1 = 3) + DF(v_2 = 0)$ collisions at
 $T = 300$ K

v_1	J_1	v_2	J_2	v'_1	J'_1	v'_2	J'_2	$\Delta E,$ cm^{-1}	k_λ^a
1	3	0	J_2	0	20	0	J_2	1427.0	1.8 ± 0.9
1	3	0	J_2	0	19	0	J_2	1010.0	3.1 ± 1.1
1	3	0	J_2	0	18	0	J_2	613.0	2.7 ± 1.1
1	3	0	J_2	0	17	0	J_2	236.0	3.4 ± 1.2
1	3	0	J_2	0	16	0	J_2	-122.0	3.2 ± 1.2
1	3	0	J_2	0	15	0	J_2	-460.0	3.7 ± 1.2
1	3	0	J_2	0	14	0	J_2	-778.0	3.6 ± 1.2
1	3	0	J_2	0	13	0	J_2	-1076.0	3.0 ± 1.2
1	3	0	J_2	0	12	0	J_2	-1353.0	4.1 ± 1.3

$a_\lambda \equiv (v_1' J_1' v_2' J_2' v'_1 J'_1 v'_2 J'_2)$. k_λ is the total rate coefficient for $v \rightarrow R$ relaxation in units of $10^{12} \text{ cm}^3/(\text{mole sec})$. To obtain rate coefficient for $v \rightarrow R$ relaxation of $DF(v_1 = 1, J_1 = 3)$ by $DF(v_2 = 0, J_2)$, multiply k_λ by $(2J_2 + 1) \exp[-(E(v_2 = 0, J_2)/kT)/Q_R(v_2, J_2)]$, where $Q_R(v_2, J_2)$ is the rotational partition function.

TABLE II. Vibrational-to-rotational detailed rate coefficients for $\text{DF}(v_1 = 2, J_1 = 3) + \text{DF}(v_2 = 0)$ collisions at $T = 300 \text{ K}$

v_1	J_1	v_2	J_2	v'_1	J'_1	v'_2	J'_2	$\Delta E, \text{cm}^{-1}$	k_λ^a
2	3	0	J_2	1	19	0	J_2	994.0	1.8 ± 0.9
2	3	0	J_2	1	18	0	J_2	608.0	4.1 ± 1.3
2	3	0	J_2	1	17	0	J_2	241.0	2.3 ± 1.0
2	3	0	J_2	1	16	0	J_2	-107.0	2.3 ± 1.0
2	3	0	J_2	1	15	0	J_2	-436.0	0.9 ± 0.6
2	3	0	J_2	1	14	0	J_2	-745.0	2.6 ± 1.0
2	3	0	J_2	1	13	0	J_2	-1035.0	2.6 ± 1.0
2	3	0	J_2	1	12	0	J_2	-1304.0	1.3 ± 0.7
2	3	0	J_2	1	11	0	J_2	-1554.0	1.8 ± 0.9
2	3	0	J_2	0	25	0	J_2	973.0	3.1 ± 1.2
2	3	0	J_2	0	24	0	J_2	465.0	4.4 ± 1.4
2	3	0	J_2	0	23	0	J_2	-25.0	1.8 ± 0.9
2	3	0	J_2	0	22	0	J_2	-497.0	3.6 ± 0.9
2	3	0	J_2	0	21	0	J_2	-950.0	3.1 ± 1.2
2	3	0	J_2	0	20	0	J_2	-1385.0	1.3 ± 0.7

$a_\lambda \equiv (v_1, J_1, v_2, J_2, v'_1, J'_1, v'_2, J'_2)$. k_λ is the total rate coefficient for $v \rightarrow R$ relaxation in units of $10^{12} \text{ cm}^3/(\text{mole sec})$. To obtain rate coefficient for $v \rightarrow R$ relaxation of $\text{DF}(v_1 = 2, J_1 = 3)$ by $\text{DF}(v_2 = 0, J_2)$, multiply by $(2J_2 + 1) \exp[-(E(v_2 = 0, J_2)/kT)]/Q_R(v_2, J_2)$, where $Q_R(v_2, J_2)$ is the rotational partition function.

TABLE III. Vibrational-to-rotational detailed rate coefficients for
 $DF(v_1 = 3, J_1 = 3) + DF(v_2 = 0)$ collisions at
 $T = 300$ K

v_1	J_1	v_2	J_2	v'_1	J'_1	v'_2	J'_2	$\Delta E, cm^{-1}$	k_λ^a
3	3	0	J_2	2	18	0	J_2	603.0	4.4 ± 1.4
3	3	0	J_2	2	17	0	J_2	246.0	2.6 ± 1.0
3	3	0	J_2	2	16	0	J_2	-92.0	2.2 ± 1.0
3	3	0	J_2	2	15	0	J_2	-412.0	3.0 ± 1.1
3	3	0	J_2	2	14	0	J_2	-712.0	1.8 ± 0.9
3	3	0	J_2	2	13	0	J_2	-994.0	2.6 ± 1.0
3	3	0	J_2	2	12	0	J_2	-1256.0	2.2 ± 1.0
3	3	0	J_2	2	11	0	J_2	-1499.0	1.8 ± 0.9
3	3	0	J_2	1	24	0	J_2	476.0	1.8 ± 0.9
3	3	0	J_2	1	23	0	J_2	0.0	1.3 ± 0.9
3	3	0	J_2	1	22	0	J_2	-459.0	3.5 ± 1.2
3	3	0	J_2	1	21	0	J_2	-900.0	1.8 ± 0.9
3	3	0	J_2	1	20	0	J_2	-1323.0	1.3 ± 0.9
3	3	0	J_2	1	19	0	J_2	-1728.0	2.2 ± 1.0
3	3	0	J_2	0	30	0	J_2	-1044.0	3.0 ± 1.1
3	3	0	J_2	0	29	0	J_2	452.0	3.5 ± 1.2
3	3	0	J_2	0	28	0	J_2	-123.0	3.5 ± 1.2
3	3	0	J_2	0	27	0	J_2	-682.0	1.3 ± 0.9
3	3	0	J_2	0	26	0	J_2	-1224.0	2.6 ± 1.0
3	3	0	J_2	0	25	0	J_2	-1749.0	1.8 ± 0.9

^a $\lambda \equiv (v_1, J_1, v_2, J'_1, v'_2, J'_2)$. k_λ is the total rate coefficient for $v \rightarrow R$ relaxation in units of $10^{12} cm^3/(mole sec)$. To obtain rate coefficient for $v \rightarrow R$ relaxation of $DF(v_1 = 3, J_1 = 3)$ by $DF(v_2 = 0, J_2)$, multiply k_λ by $(2J_2 + 1) \exp[-(E(v_2 = 0, J_2)/kT)]/Q_R(v_2, J_2)$, where $Q_R(v_2, J_2)$ is the rotational partition function.

double, since a quantum of vibrational energy for DF is slightly less than 75% that of a quantum of vibrational energy for HF. For example, a loss of three quanta of vibrational energy from HF* is sufficient to form an HF(v = 0, J = 24) molecule, with an energy defect of 125 cm^{-1} (see Ref. 5). In DF*-DF collisions, a loss of three quanta of vibrational energy from DF* is sufficient to form a DF(v = 0, J = 28) molecule with an energy-defect of -123 cm^{-1} (Table III). As shown in Table III, when a DF(v = 3) molecule collides with a DF(v = 0) molecule, the DF(v = 3) molecule can convert one, two, or three quanta of vibrational energy into rotational energy of the same DF molecule by way of an intramolecular energy-transfer mechanism. When both DF molecules are vibrationally excited (Tables IV and V), either or both DF molecules can convert one or more quanta of vibrational energy of either or both DF* molecules by intramolecular energy transfer. The $v \rightarrow R$ processes predicted in this study for DF*-DF collisions and in a previous study for HF*-HF collisions can be used to explain the high J-states observed in the pure rotational laser described by Deutsch.¹⁴ Krogh and Pimentel¹⁵ have observed stimulated vibration-rotation emission from HF with high rotational excitation following flash photolysis of $\text{ClF}_x\text{-H}_2\text{-Ar}$ mixtures. Their study indicated that the pattern of emission rules out direct population of the high J-states by the vibrational pumping reaction(s) and is not consistent with Boltzmann equilibration. Krogh and Pimentel concluded that their results point to an energy-transfer mechanism that involves rapid $v \rightarrow R$ deactivation with large ΔJ change coupled with $v \rightarrow v$ pumping in HF*-HF* collisions.

In Tables IV through VI are listed detailed rate coefficients $k_{v_1, v_2, v_1', v_2'}$ at $T = 300 \text{ K}$ for the $v \rightarrow R$ energy-transfer processes $\text{DF}(v_1) + \text{DF}(v_2) \rightarrow \text{DF}(v_1') + \text{DF}(v_2')$. The overall rate coefficients k_{vR} tabulated in Tables IV through VI indicate a slight increase with increasing v . The $v \rightarrow R$ rate coefficients $k_{v_1, v_2, v_1', v_2'}$ are converted to probabilities $P_{v_1, v_2, v_1', v_2'}$ by dividing $k_{v_1, v_2, v_1', v_2'}$ by the gas kinetic rate $8.8 \times 10^{13} \text{ cm}^3/(\text{mole sec})$ at room temperature.

TABLE IV. Rate coefficients $k_{v_1, v_2; v'_1, v'_2}$ for vibrational-to-rotational energy transfer in $\text{DF}(v_1) + \text{DF}(v_2)$ collisions at $T = 300$ K.

v_1	v_2	v'_1	v'_2	$k_{v_1, v_2; v'_1, v'_2}$	k_{vR}^a
1	1	1	0	4.0 ± 0.3	
1	1	0	0	0.6 ± 0.2	4.6 ± 0.3
2	2	2	1	2.7 ± 0.3	
2	2	2	0	1.4 ± 0.2	
2	2	1	1	0.7 ± 0.2	
2	2	1	0	0.9 ± 0.2	
2	2	0	0	0.4 ± 0.1	6.1 ± 0.3
3	3	3	2	2.0 ± 0.3	
3	3	3	1	1.0 ± 0.2	
3	3	3	0	1.0 ± 0.2	
3	3	2	2	0.3 ± 0.1	
3	3	2	1	0.9 ± 0.2	
3	3	2	0	0.6 ± 0.1	
3	3	1	1	0.3 ± 0.1	
3	3	1	0	0.1 ± 0.1	
3	3	0	0	0.1 ± 0.1	6.4 ± 0.3
4	4	4	3	2.1 ± 0.4	
4	4	4	2	1.5 ± 0.3	
4	4	4	1	0.3 ± 0.2	
4	4	4	0	0.7 ± 0.2	
4	4	3	3	0.5 ± 0.2	
4	4	3	2	0.3 ± 0.2	
4	4	3	1	0.5 ± 0.2	
4	4	3	0	0.5 ± 0.2	
4	4	2	2	0.1 ± 0.1	
4	4	2	1	0.1 ± 0.1	
4	4	2	0	0.1 ± 0.1	
4	4	1	1	0.3 ± 0.2	
4	4	0	1	0.1 ± 0.1	
4	4	0	0	0.1 ± 0.1	7.2 ± 0.3
5	5	5	4	1.6 ± 0.2	
5	5	5	3	1.0 ± 0.2	
5	5	5	2	0.6 ± 0.2	
5	5	5	1	0.8 ± 0.2	
5	5	5	0	0.7 ± 0.2	
5	5	4	4	0.4 ± 0.1	
5	5	4	3	0.4 ± 0.1	
5	5	4	2	0.1 ± 0.1	
5	5	4	1	0.3 ± 0.1	
5	5	4	0	0.3 ± 0.1	
5	5	3	3	0.3 ± 0.1	
5	5	3	2	0.3 ± 0.1	
5	5	3	1	0.3 ± 0.1	
5	5	3	0	0.2 ± 0.1	
5	5	2	2	0.1 ± 0.1	
5	5	2	1	0.1 ± 0.1	
5	5	2	0	0.4 ± 0.1	
5	5	1	1	0.1 ± 0.1	
5	5	1	0	0.1 ± 0.1	
5	5	0	0	0.1 ± 0.1	8.0 ± 0.4

^a $k_{v_1, v_2; v'_1, v'_2}$ is in units of $10^{13} \text{ cm}^3 / (\text{mole sec})$.

TABLE V. Rate coefficient $k_{v_1, v_2; v'_1, v'_2}$ for vibrational-to-rotational energy transfer in $\text{DF}(v_1) + \text{DF}(v_2)$ collisions at $T = 300$ K.

v_1	v_2	v'_1	v'_2	$k_{v_1, v_2; v'_1, v'_2}$	k_{vR}^a
2	1	1	1	1.7 ± 0.2	
2	1	0	1	1.5 ± 0.2	
2	1	2	0	1.6 ± 0.2	
2	1	0	0	0.5 ± 0.1	5.3 ± 0.3
3	1	2	1	1.4 ± 0.2	
3	1	1	1	0.7 ± 0.2	
3	1	0	1	1.2 ± 0.2	
3	1	3	0	1.3 ± 0.2	
3	1	2	0	0.7 ± 0.2	
3	1	0	0	0.4 ± 0.1	5.7 ± 0.3
4	1	3	1	1.3 ± 0.2	
4	1	2	1	0.9 ± 0.2	
4	1	1	1	0.6 ± 0.2	
4	1	0	1	0.9 ± 0.2	
4	1	4	0	1.3 ± 0.2	
4	1	3	0	0.5 ± 0.2	
4	1	2	0	0.2 ± 0.1	
4	1	0	0	0.4 ± 0.1	6.1 ± 0.3
5	1	4	1	1.1 ± 0.2	
5	1	3	1	0.7 ± 0.2	
5	1	2	1	0.7 ± 0.2	
5	1	1	1	0.5 ± 0.2	
5	1	0	1	0.5 ± 0.2	
5	1	5	0	1.1 ± 0.2	
5	1	4	0	0.5 ± 0.2	
5	1	3	0	0.4 ± 0.1	
5	1	2	0	0.4 ± 0.1	
5	1	0	0	0.3 ± 0.1	6.2 ± 0.1

^a $k_{v_1, v_2; v'_1, v'_2}$ is in units of $10^{13} \text{ cm}^3/(\text{mole sec})$.

TABLE VI. Rate coefficients $k_{v_1' v_2; v_1' v_2'}$ for vibrational-to-rotational energy transfer in $\text{DF}(v_1) + \text{DF}(v_2)$ collisions at $T = 300$ K.

$v_1' + v_2'$	$v_1 + v_2$	$5 + 0$	$4 + 0$	$3 + 0$	$2 + 0$	$1 + 0$	$0 + 0$	Overall Rate Coefficients, b
6 + 0	19.8 ± 2.6	5.7 ± 1.5	6.6 ± 1.6	6.2 ± 1.6	7.0 ± 1.7	8.8 ± 1.9	54.1 ± 3.0	
5 + 0		15.8 ± 2.4	13.6 ± 2.2	10.1 ± 2.0	4.4 ± 1.4	8.8 ± 1.9	52.7 ± 3.0	
4 + 0			18.9 ± 2.6	11.9 ± 2.1	11.0 ± 2.1	7.5 ± 1.7	49.3 ± 3.1	
3 + 0				20.6 ± 2.6	11.9 ± 2.0	15.7 ± 2.4	48.2 ± 3.1	
2 + 0					19.7 ± 2.6	17.3 ± 2.5	37.0 ± 3.1	
1 + 0						28.6 ± 1.5	28.6 ± 1.5	

a $k_{v_1' v_2; v_1' v_2'}$ is in units of $10^{12} \text{ cm}^3 / (\text{mole sec})$.

b The overall rate coefficient is the summation of $k_{v_1' v_2; v_1' v_2'}$ over the v_1' levels.

It can be calculated from Table VI that there is a probability of 0.2 for most single-quantum transitions and a probability of 0.1 for most multiquantum transitions from a given vibrational level ($v > 1$). As shown in Tables IV through VI, there is an increase in the number of $v \rightarrow R$ channels and a decrease in the specific rate coefficients for $v \rightarrow R$ processes with increasing v . The multiquantum $v \rightarrow R$ energy-transfer processes in DF*-DF collisions are slightly less probable than the single-quantum transitions. Similar conclusions were predicted by Wilkins⁵ for HF*-HF collisions. The overall rate coefficients presented in Tables IV through VI are not comparable to the effective quenching-rate coefficients measured in the laboratory. This study shows that, as in DF*-DF collisions, rotational up-pumping occurs as the vibrational energy of the DF* molecule is reduced by deactivation.

B. VIBRATIONAL-TO-VIBRATIONAL ENERGY TRANSFER

In Table VII are tabulated rate coefficients for room-temperature $v \rightarrow v$ energy-transfer processes obtained from this trajectory study. Rate coefficients were calculated for both the endothermic and exothermic $v \rightarrow v$ energy-transfer processes. In column 6 is given the energy mismatch ΔE obtained from the relationship between the rate coefficients for the endothermic and exothermic processes, i. e., $k(\text{exo}) = k(\text{endo}) \cdot \exp(\Delta E/RT)$. In DF + DF collisions, the $v \rightarrow v$ processes are very much near-resonant. In column 7 is listed the energy mismatch obtained under the assumption that both reagent and product DF molecules have zero rotational energy. This trajectory study indicates that rotational states of reagent and product DF species must be considered in order to calculate a realistic energy-defect ΔE . The rate coefficients for $v \rightarrow v$ exchange decrease with v for both the endothermic and exothermic $v \rightarrow v$ energy-transfer processes. From this trajectory study, it is predicted that only single-quantum transitions are important in the $v \rightarrow v$ intermolecular energy-transfer processes. The v -dependence of the rate coefficients for $v \rightarrow v$ processes in the exothermic direction is given by $k(v_1 = 1, v_2; v'_1 = 0, v'_2 = v_2 + 1) = (1.61)^{1-v_2} k(v_1 = 1, v_2 = 1; v'_1 = 0, v'_2 = 2)$ with $v_2 = 1$ through 5 and where, at room temperature,

TABLE VII. Rate coefficients for vibrational-to-vibrational energy transfer. $\text{DF}(\nu_1) + \text{DF}(\nu_2) \rightarrow \text{DF}(\nu_1 - 1) + \text{DF}(\nu_2 + 1)$.

ν_1	ν_2	$\nu_1 - 1$	$\nu_2 + 1$	$k_{\nu_1, \nu_2; \nu_1 - 1, \nu_2 + 1}$ $10^{12} \text{ cm}^3 / (\text{mole sec})$	$\Delta E, \text{ b}$ cm^{-1}	$\Delta E, \text{ c}$ cm^{-1}
2	0	1	1	10.6 ± 2.0	46.0	91.0
3	0	2	1	6.5 ± 1.5	58.0	182.0
4	0	3	1	4.1 ± 1.4	61.0	269.0
5	0	4	1	2.2 ± 1.2	71.0	357.0
6	0	5	1	1.2 ± 0.8	84.0	441.0
1	1	0	2	13.2 ± 2.2	-46.0	-91.0
1	2	0	3	8.6 ± 1.8	-58.0	-182.0
1	3	0	4	5.5 ± 1.4	-61.0	-269.0
1	4	0	5	3.1 ± 1.2	-71.0	-357.0
1	5	0	6	1.8 ± 0.9	-84.0	-441.0
2	2	1	3	4.8 ± 1.4	-	-91.0
3	3	2	4	3.5 ± 1.2	-	-87.0
4	4	3	5	3.1 ± 1.5	-	-87.0
5	5	4	6	1.8 ± 0.9	-	-84.0
6	6	5	7	0.9 ± 0.3	-	-80.0

a $T = 300 \text{ K}$. The value in the table must be multiplied by $(T/300)^{0.5}$ to obtain rate coefficient at any other temperature.

b Trajectory calculations.

c Change in rotational energy across reaction is assumed to be zero.

$k(v_1 = 1, v_2 = 1; v'_1 = 0, v'_2 = 2) = 1.3 \times 10^{13} \text{ cm}^3/(\text{mole sec})$. Ernst, Osgood, and Javan² reported $1.1 \times 10^{13} \text{ cm}^3/(\text{mole sec})$ for the endothermic reaction $\text{DF}(v_1 = 2) + \text{DF}(v_1 = 0) \rightarrow \text{DF}(v'_1 = 1) + \text{DF}(v'_2 = 1)$. This value compares favorably with our value $k(v_1 = 2, v_2 = 0, v'_1 = 1, v'_2 = 1) = 1.1 \times 10^{13} \text{ cm}^3/(\text{mole sec})$, which is given in Table VII. Bott's¹ room-temperature value for this endothermic reaction is approximately 15% higher. The $v \rightarrow v$ rates are predicted to be faster in $\text{DF}(v_1) + \text{DF}(v_2)$ collisions than in $\text{HF}(v_1) + \text{HF}(v_2)$ collisions. Experimental measurements confirm this conclusion. Measurements on the higher vibrational levels have not been reported. Trajectory calculations were completed for $T = 300, 500, 1000$, and 1500 K . Analysis of the detailed rate coefficients indicate a temperature dependence of $T^{0.5}$ for both the $v \rightarrow v$ and $v \rightarrow R$ energy-transfer processes. The slow $v \rightarrow v$ pumping rates and the fast $v \rightarrow R$ deactivation rates with increasing v account for the large decrease in measured HF or DF species concentrations observed in the higher vibrational levels of HF or DF chemical lasers.

C. ROTATIONAL-TO-ROTATIONAL-TRANSLATIONAL ENERGY TRANSFER

The rate coefficients for rotational relaxation by $R \rightarrow T$ energy transfer from highly rotationally excited HF molecules were found^{5, 16, 17} to decrease with increasing J . This decrease is expected, since an increase in J is associated with an increase in the energy spacings between rotational levels. In addition, collisions with resonance transfer of rotational energy, i.e., $R \rightarrow R'$ energy transfer, play an important role in rotational deactivation. The rotational energy given up by one HF molecule is transferred to its partner in collision. The $R \rightarrow (R', T)$ energy-transfer processes in $\text{HF} + \text{HF}$ or $\text{DF} + \text{DF}$ collisions provide the drainage necessary for the rotational non-equilibrium states to relax to their thermal distributions.

The rate coefficients for rotational relaxation of $\text{DF}(v_1 = 0, J_1 = 5, 10, 15, \text{ and } 20)$ by $\text{DF}(v_2 = 0, J_2)$ molecules are shown in Figs. 1 through 4. Contributions from both $R \rightarrow R'$ and $R \rightarrow T$ energy-transfer processes are included in these rate coefficients. The $R \rightarrow T$ mechanism with $\Delta J = -1$ is

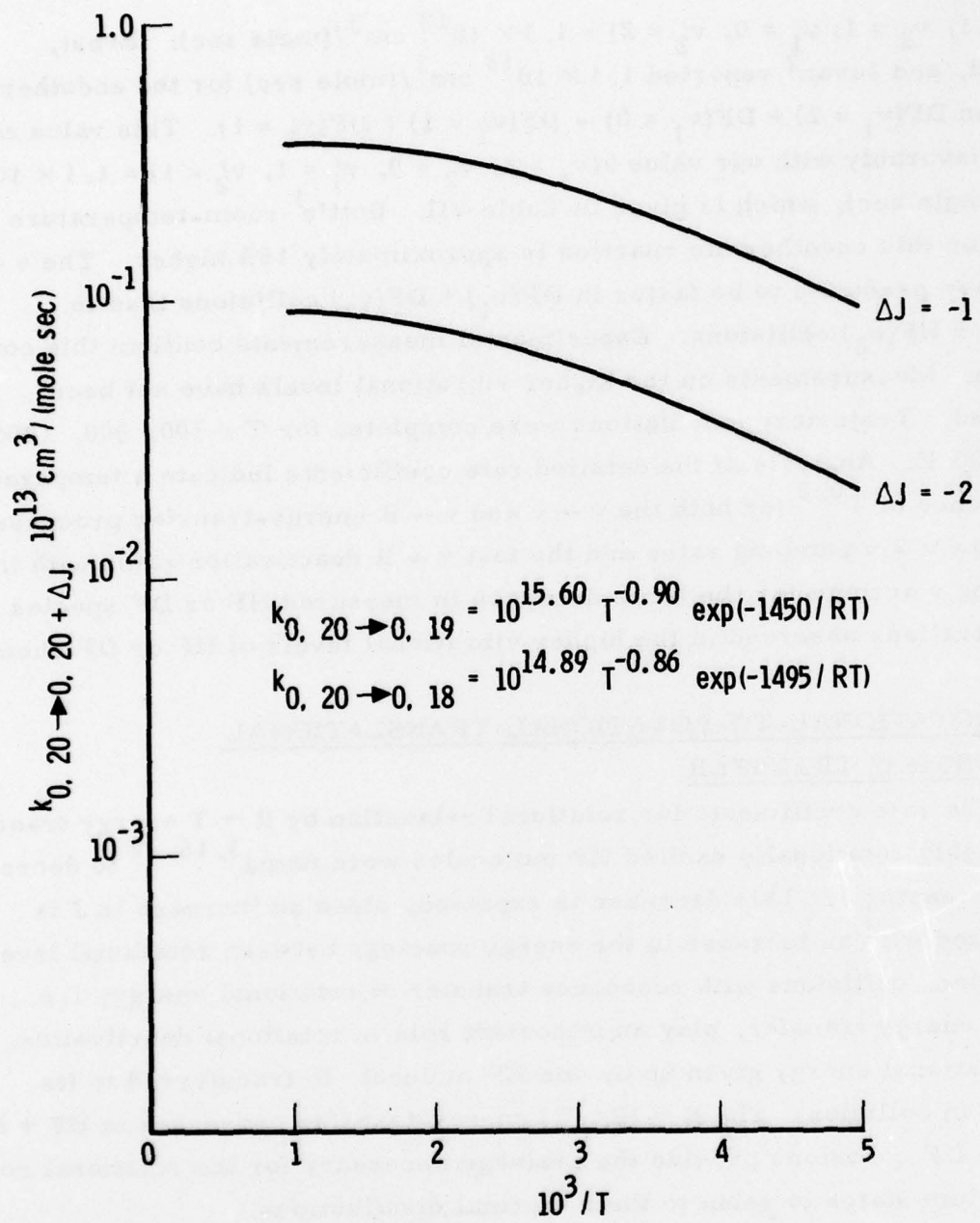


Figure 1. Rate Coefficients for $R \rightarrow (R', T)$ Energy Transfer of $DF(v = 0, J = 20)$ by $DF(v_2 = 0, J_2)$ vs $10^3/T$

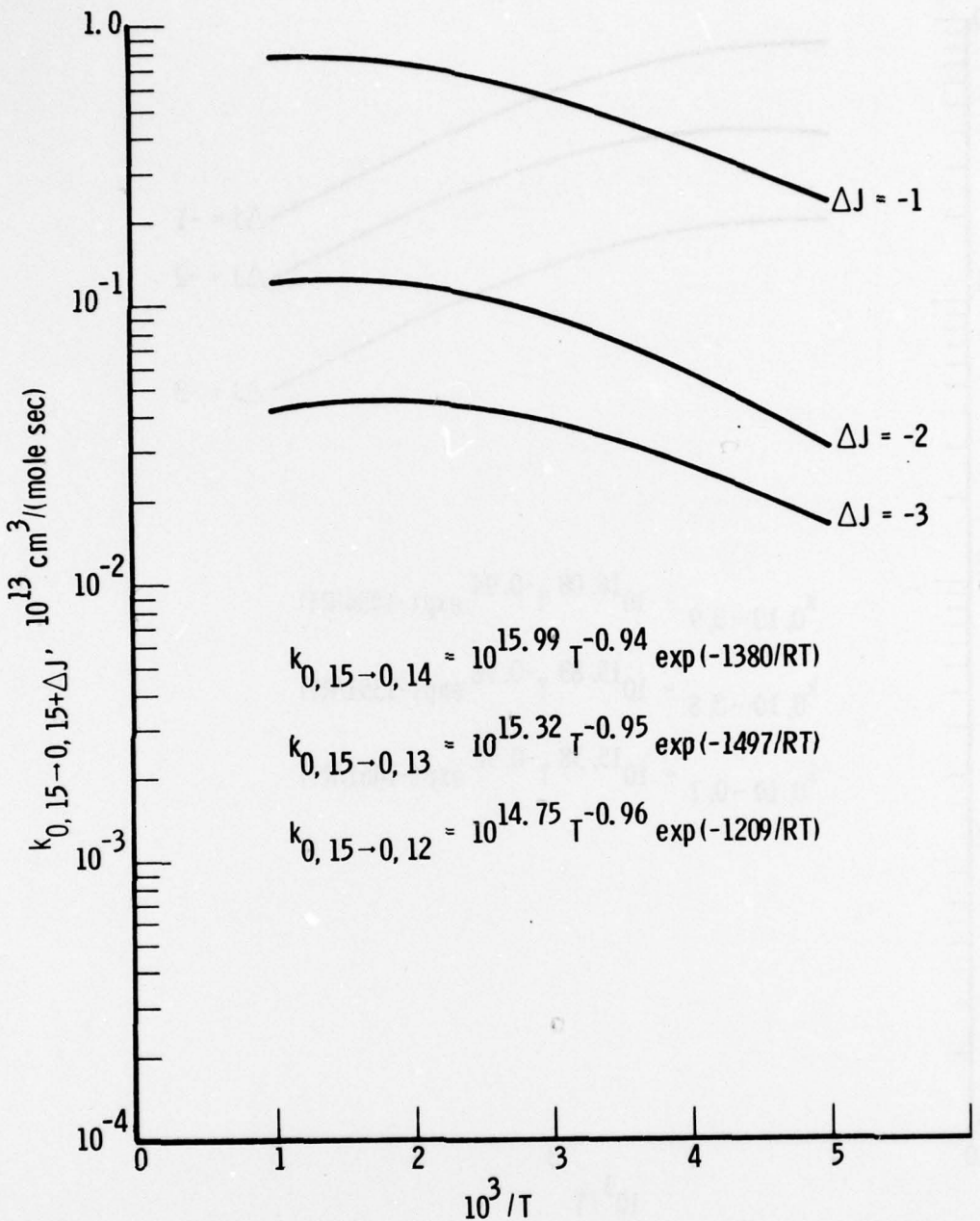


Figure 2. Rate Coefficients for $R \rightarrow (R', T)$ Energy Transfer of $DF(v_1 = 0, J = 15)$ by $DF(v_2 = 0, J_2)$ vs $10^3/T$

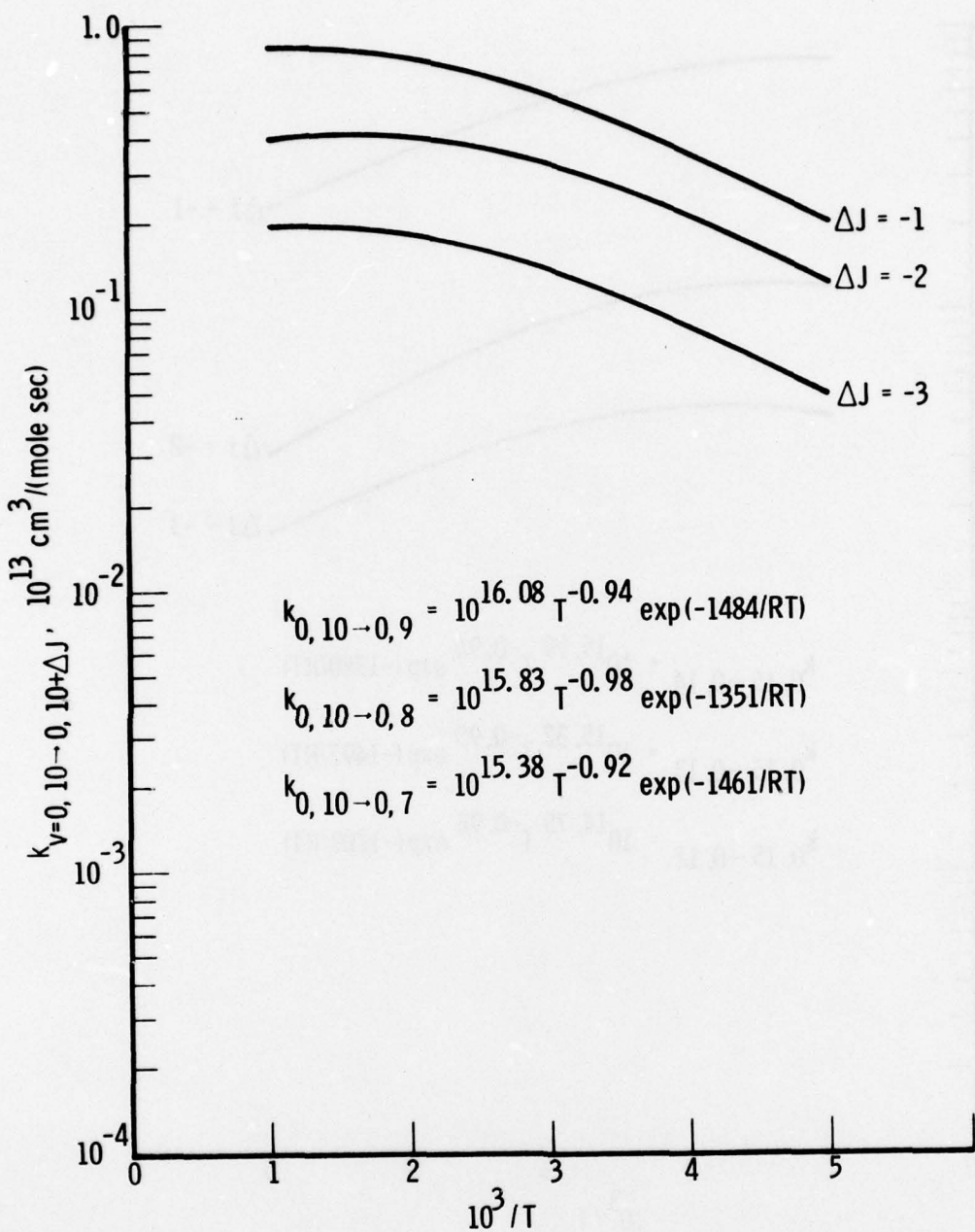


Figure 3. Rate Coefficients for $R \rightarrow (R', T)$ Energy Transfer of $DF(v_1 = 0, J_1 = 10)$ by $DF(v_2 = 0, J_2)$ vs $10^3/T$

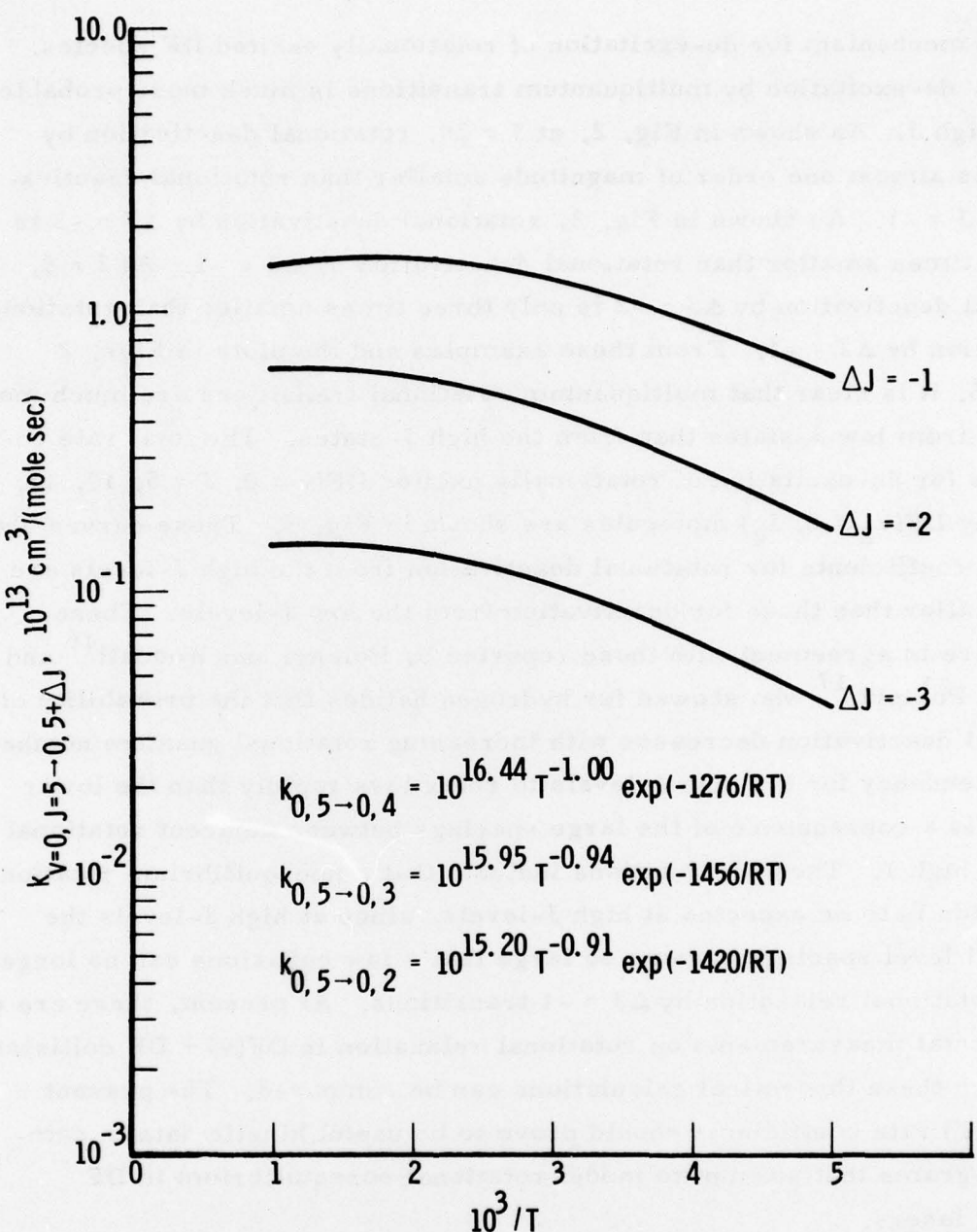


Figure 4. Rate Coefficients for $R \rightarrow (R', T)$ Energy Transfer of $DF(v_1 = 0, J_1 = 5)$ by $DF(v_2 = 0, J_2)$ vs $10^3/T$

the main mechanism for de-excitation of rotationally excited DF species. At low J , de-excitation by multiquantum transitions is much more probable than at high J . As shown in Fig. 2, at $J = 20$, rotational deactivation by $\Delta J = -2$ is almost one order of magnitude smaller than rotational deactivation by $\Delta J = -1$. As shown in Fig. 3, rotational deactivation by $\Delta J = -3$ is about 20 times smaller than rotational deactivation by $\Delta J = -1$. At $J = 5$, rotational deactivation by $\Delta J = -2$ is only three times smaller than rotational deactivation by $\Delta J = -1$. From these examples and the plots in Figs. 2 through 5, it is clear that multiquantum rotational transitions are much more probable from low J -states than from the high J -states. The total rate coefficients for de-excitation of rotationally excited $DF(v = 0, J = 5, 10, 15, \text{ and } 20)$ by $DF(v_2 = 0, J_2)$ molecules are shown in Fig. 5. These curves show that rate coefficients for rotational deactivation from the high J -levels are much smaller than those for deactivation from the low J -levels. These results are in agreement with those reported by Polanyi and Woodall¹⁶ and Ding and Polanyi,¹⁷ who showed for hydrogen halides that the probability of rotational deactivation decreases with increasing rotational quantum number J . The tendency for the high J -levels to relax less rapidly than the lower J -levels is a consequence of the large spacings between adjacent rotational states of high J . These calculations indicate that a nonequilibrium rotational distribution is to be expected at high J -levels, since at high J -levels the rotational level spacings become so large that a few collisions can no longer induce rotational relaxation by $\Delta J = -1$ transitions. At present, there are no experimental measurements on rotational relaxation in $DF(v) + DF$ collisions with which these theoretical calculations can be compared. The present $R \rightarrow (R', T)$ rate coefficients should prove to be useful kinetic data in computer programs that attempt to model rotational nonequilibrium in DF chemical lasers.

D. VIBRATIONAL RELAXATION OF $DF(v_1 = 1)$ BY $DF(v_2 = 0)$

The detailed rate coefficients for the $v \rightarrow R$ energy-transfer processes listed in Table I, together with the $R \rightarrow (R', T)$ rate coefficients presented in

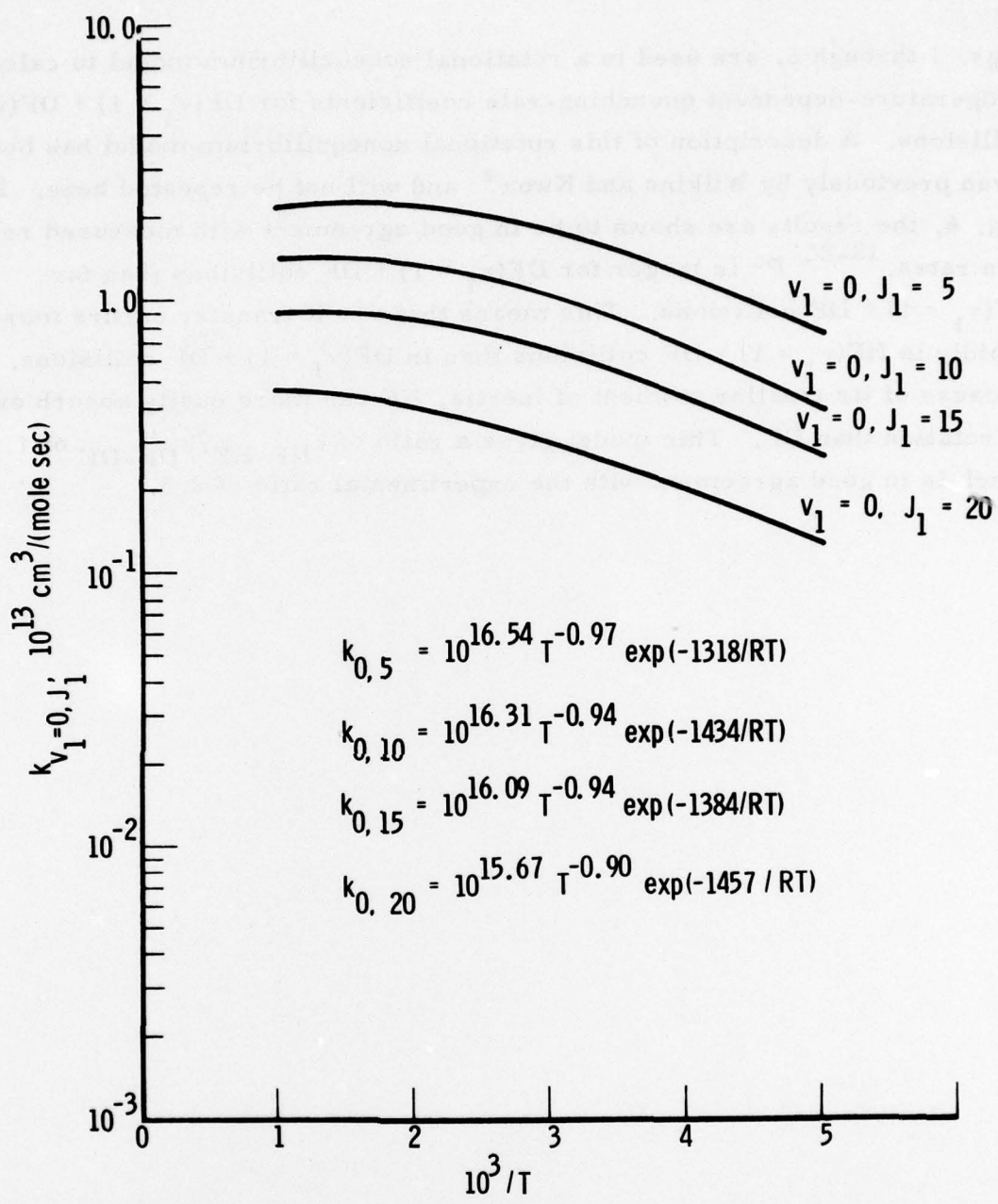


Figure 5. Total Rate Coefficients for Rotational Deactivation of DF($v_1 = 0, J_1 = 5, 10, 15$, and 20) by DF($v_2 = 0, J_2$)

Figs. 1 through 5, are used in a rotational nonequilibrium model to calculate temperature-dependent quenching-rate coefficients for $DF(v_1 = 1) + DF(v_2 = 0)$ collisions. A description of this rotational nonequilibrium model has been given previously by Wilkins and Kwok* and will not be repeated here. In Fig. 6, the results are shown to be in good agreement with measured relaxation rates.¹⁸⁻²⁴ $P\tau$ is larger for $DF(v_1 = 1) + DF$ collisions than for $HF(v_1 = 1) + HF$ collisions. This means that $v \rightarrow R$ transfer occurs more rapidly in $HF(v_1 = 1) + HF$ collisions than in $DF(v_1 = 1) + DF$ collisions. Because of its smaller moment of inertia, HF can more easily absorb energy as rotation than DF. This model gives a ratio of k_{HF-HF}/k_{DF-DF} of 1.8, which is in good agreement with the experimental ratio of 2.3.

* R. L. Wilkins and M. A. Kwok, "Temperature Dependence of Hydrogen Fluoride Vibrational Relation" (to be published).



Figure 6. Vibrational Relaxation of $\text{DF}(v_1 = 1)$ by $\text{DF}(v_2 = 0)$. P vs T and $T^{-1/3}$

REFERENCES

1. J. F. Bott, Chem. Phys. Lett. 23, 335 (1973).
2. K. Ernst, R. M. Osgood, Jr., and A. Javan, Chem. Phys. Lett. 23, 553 (1973).
3. Ian W. M. Smith, Vibrational Relaxation Rates for HF(v ≤ v ≤ 7) and DF(v ≤ v ≤ 5), final report prepared for Office of Naval Research, Contract No. N0014-74-C-0421 (July 1976).
4. M. A. Kwok, Progress in the Study of Collisional Quenching of DF(v ≤ 8) by Use of a Large Flow Tube, TR-0077(2603)-4, The Aerospace Corporation, El Segundo, California (18 August 1977).
5. R. L. Wilkins, J. Chem. Phys. 67, 5838 (1977).
6. D. R. Yarkony, S. V. O'Neil, H. F. Schaefer III, G. P. Baskin, and C. F. Bender, J. Chem. Phys. 60, 855 (1974).
7. G. A. Parker, R. L. Snow, and R. T. Pack, Chem. Phys. Lett. 33, 399 (1975).
8. L. M. Raff, D. L. Thompson, L. B. Sims, and R. N. Porter, J. Chem. Phys. 56, 5998 (1972).
9. R. N. Porter, L. M. Raff, and W. H. Miller, J. Chem. Phys. 63, 2214 (1975).
10. S. Gill, Proc. Cambridge Phil. Soc. 47, 96 (1951).
11. J. T. Muckerman, J. Chem. Phys. 54, 1155 (1971).
12. R. L. Wilkins, J. Chem. Phys. 59, 698 (1973).
13. M. Karplus, R. N. Porter, and R. D. Sharma, J. Chem. Phys. 43, 3239 (1965).
14. T. F. Deutsch, Appl. Phys. Lett. 11, 18 (1967).
15. O. D. Krogh and G. C. Pimentel, J. Chem. Phys. 67, 2993 (1977).
16. J. C. Polanyi and K. B. Woodall, J. Chem. Phys. 56, 1563 (1972).
17. A. M. G. Ding and J. C. Polanyi, Chem. Phys. Lett. 10, 39 (1975)

18. J. F. Bott and N. Cohen, *J. Chem. Phys.* 58, 934 (1973); 59, 447 (1973).
19. J. A. Blauer, W. C. Solomon, and T. W. Owens, *Int. J. Chem. Kinet.* 4, 293 (1972).
20. G. K. Vasil'ev, E. F. Makarov, V. G. Papin, and V. L. Tal'roze, *Zh. Eksp. Teor. Fiz.* 64, 2046 (1973).
21. R. R. Stephens and T. A. Cool, *J. Chem. Phys.* 56, 5863 (1972).
22. J. J. Hinchen, *J. Chem. Phys.* 59, 233 (1973); 59, 2224 (1973).
23. R. A. Lucht and T. A. Cool, *J. Chem. Phys.* 60, 1026 (1974).
24. J. L. Ahl and T. A. Cool, *J. Chem. Phys.* 58, 5540 (1973).

THE IVAN A. GETTING LABORATORIES

The Laboratory Operations of The Aerospace Corporation is conducting experimental and theoretical investigations necessary for the evaluation and application of scientific advances to new military concepts and systems. Versatility and flexibility have been developed to a high degree by the laboratory personnel in dealing with the many problems encountered in the nation's rapidly developing space and missile systems. Expertise in the latest scientific developments is vital to the accomplishment of tasks related to these problems. The laboratories that contribute to this research are:

Aerophysics Laboratory: Launch and reentry aerodynamics, heat transfer, reentry physics, chemical kinetics, structural mechanics, flight dynamics, atmospheric pollution, and high-power gas lasers.

Chemistry and Physics Laboratory: Atmospheric reactions and atmospheric optics, chemical reactions in polluted atmospheres, chemical reactions of excited species in rocket plumes, chemical thermodynamics, plasma and laser-induced reactions, laser chemistry, propulsion chemistry, space vacuum and radiation effects on materials, lubrication and surface phenomena, photo-sensitive materials and sensors, high precision laser ranging, and the application of physics and chemistry to problems of law enforcement and biomedicine.

Electronics Research Laboratory: Electromagnetic theory, devices, and propagation phenomena, including plasma electromagnetics; quantum electronics, lasers, and electro-optics; communication sciences, applied electronics, semiconducting, superconducting, and crystal device physics, optical and acoustical imaging; atmospheric pollution; millimeter wave and far-infrared technology.

Materials Sciences Laboratory: Development of new materials; metal matrix composites and new forms of carbon; test and evaluation of graphite and ceramics in reentry; spacecraft materials and electronic components in nuclear weapons environment; application of fracture mechanics to stress corrosion and fatigue-induced fractures in structural metals.

Space Sciences Laboratory: Atmospheric and ionospheric physics, radiation from the atmosphere, density and composition of the atmosphere, aurorae and airglow; magnetospheric physics, cosmic rays, generation and propagation of plasma waves in the magnetosphere; solar physics, studies of solar magnetic fields; space astronomy, x-ray astronomy; the effects of nuclear explosions, magnetic storms, and solar activity on the earth's atmosphere, ionosphere, and magnetosphere; the effects of optical, electromagnetic, and particulate radiations in space on space systems.

THE AEROSPACE CORPORATION
El Segundo, California